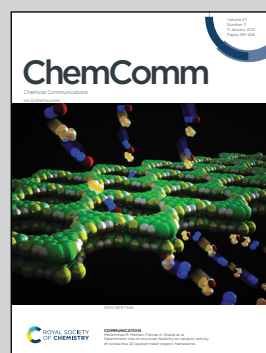


**Showcasing research from Professor Kudo's laboratory,
Department of Applied Chemistry, Tokyo University of
Science, Tokyo, Japan.**

Highly crystalline $\text{Na}_{0.5}\text{Bi}_{0.5}\text{TiO}_3$ of a photocatalyst
valence-band-controlled with Bi(III) for solar water splitting

A highly crystalline $\text{Na}_{0.5}\text{Bi}_{0.5}\text{TiO}_3$ powder with a perovskite
structure was successfully synthesized using a NaCl -flux
method. The powdered photocatalyst in which the valence
band consisted of Bi(III) showed a 5.1% apparent quantum
yield at 350 nm for water splitting.

As featured in:



See Akihiko Kudo *et al.*,
Chem. Commun., 2021, **57**, 323.



Cite this: *Chem. Commun.*, 2021, 57, 323

Received 9th November 2020,
Accepted 7th December 2020

DOI: 10.1039/d0cc07371g

rsc.li/chemcomm

Highly crystalline $\text{Na}_{0.5}\text{Bi}_{0.5}\text{TiO}_3$ of a photocatalyst valence-band-controlled with Bi(III) for solar water splitting†

Kenta Watanabe,^a Yoichi Iikubo,^a Yuichi Yamaguchi^{ab} and Akihiko Kudo^{ab}

$\text{Na}_{0.5}\text{Bi}_{0.5}\text{TiO}_3$ (BG 3.1 eV) with a valence band formed by Bi(III) was found as a new photocatalyst for solar water splitting. The water splitting activity of highly crystalline $\text{Na}_{0.5}\text{Bi}_{0.5}\text{TiO}_3$ synthesized by a flux method was much higher than that of the samples synthesized by a solid-state reaction. The optimized RhCr_2O_x (0.1 mol%)/ $\text{Na}_{0.5}\text{Bi}_{0.5}\text{TiO}_3$ /CoOOH (0.02 mol%) gave a 5.1% apparent quantum yield at 350 nm and split water even under simulated sunlight irradiation with a 0.05% solar to hydrogen energy conversion efficiency. We have successfully achieved solar water splitting using a one-step photoexcitation type photocatalyst valence-band-controlled with Bi(III).

Hydrogen production by photocatalytic solar water splitting is attractive, and important science and technology from the viewpoint of resource, energy and environmental issues. Therefore, many researchers have developed various powder-based visible-light-driven photocatalysts working by a one-step photoexcitation and a Z-schematic two-step photoexcitation for water splitting.^{1–6} The one-step photoexcitation type photocatalyst especially possesses an advantage in practical use from the viewpoint of its simplicity. Domen and co-workers have reported that GaN–ZnO,⁷ ZnGeN₂–ZnO,⁸ LaMg_{1/3}Ta_{2/3}O₂N,⁹ TaON,¹⁰ CaTaO₂N,¹¹ Ta₃N₅¹² and Y₂Ti₂O₅S₂¹³ of (oxy)nitride and oxysulfide photocatalysts show activities for one-step photoexcitation type water splitting under visible light irradiation. It is also reported that g-C₃N₄ of an organic semiconductor photocatalyst can split water under visible light irradiation.¹⁴ We have also reported that IrO₂-loaded SrTiO₃ co-doped with Rh and Sb of a metal oxide photocatalyst shows activity for water splitting under visible light irradiation.¹⁵ Although some

of these visible-light-driven photocatalysts can split water under simulated sunlight irradiation, their solar to hydrogen energy conversion efficiencies (STH) are still low due to their low apparent quantum yields (AQYs). In recent years, Domen and co-workers have developed an Al-doped SrTiO₃ (band gap (BG) 3.2 eV) photocatalyst loading Rh/Cr₂O₃ and CoOOH cocatalysts with almost 100% AQY, which was prepared by a flux treatment.¹⁶ Although the photocatalyst responds to only UV light, it shows the highest STH (0.65%) among one-step photoexcitation type photocatalysts.¹⁶ We have also reported that Rh_{0.5}Cr_{1.5}O₃-loaded AgTaO₃ (BG 3.4 eV) shows high AQY (38% at 340 nm) and STH (0.13%) for water splitting.¹⁷ The valence band maximum (VBM) of the Al-doped SrTiO₃ is formed by O2p orbitals, while that of AgTaO₃ is formed by Ag4d orbitals.¹⁸ A photocatalyst whose valence band (VB) is formed by orbitals of elements except oxygen like AgTaO₃ is called a valence-band (VB)-controlled photocatalyst.^{3,17,19} The VB-controlled photocatalyst is very important from the viewpoint of extension of responsive wavelength. Although the STH of the Rh_{0.5}Cr_{1.5}O₃-loaded AgTaO₃ is the highest among the VB-controlled photocatalysts, the BG of the AgTaO₃ is wider than that of the Al-doped SrTiO₃. Therefore, it is important to achieve solar water splitting with high STH using a VB-controlled photocatalyst with a narrower BG than the Al-doped SrTiO₃.

$\text{Na}_{0.5}\text{Bi}_{0.5}\text{TiO}_3$ (BG 3.1 eV) with a perovskite structure is one of the candidates satisfying the conditions mentioned above, because Bi(III) is a suitable cation for the VB-controlled photocatalyst, as seen in BiVO₄, Na_{0.5}Bi_{0.5}WO₄ and Bi₄Ti₃O₁₂.^{20–22} The VB of Na_{0.5}Bi_{0.5}TiO₃ is formed by hybridized orbitals consisting of O2p and Bi6s, leading to the narrower BG than SrTiO₃.²³ Na_{0.5}Bi_{0.5}TiO₃ showed activities for photocatalytic H₂ and O₂ evolution from aqueous solutions containing sacrificial reagents under UV irradiation as half reactions of water splitting.^{24,25} Na_{0.5}Bi_{0.5}TiO₃ photocatalysts have also been used for degradation of dyes.^{26,27} However, water splitting into H₂ and O₂ at a stoichiometric ratio over the Na_{0.5}Bi_{0.5}TiO₃ has not been achieved yet. The distortion of the perovskite framework in the crystal structure of Na_{0.5}Bi_{0.5}TiO₃ is similar to that of

^a Department of Applied Chemistry, Faculty of Science, Tokyo University of Science, 1-3 Kagurazaka, Shinjuku-ku, Tokyo 162-8601, Japan. E-mail: a-kudo@rs.tus.ac.jp

^b Photocatalysis International Research Center, Research Institute for Science and Technology, Tokyo University of Science, 2641 Yamazaki Noda-Shi, Chiba-ken 278-8510, Japan

† Electronic supplementary information (ESI) available: Experimental detail, crystal structure, XRD, XRF, XPS, DRS and a time course of an activity. See DOI: 10.1039/d0cc07371g



AgTaO₃ (Fig. S1 and Table S1, ESI†). Therefore, Na_{0.5}Bi_{0.5}TiO₃ is expected to possess potential for photocatalytic water splitting. Moreover, the activity of Na_{0.5}Bi_{0.5}TiO₃ will be improved by changing the synthesis method from a conventional solid state reaction to a flux method as well as that of SrTiO₃²⁸ because Na_{0.5}Bi_{0.5}TiO₃ is similar to SrTiO₃ from the viewpoints of a perovskite structure consisting of TiO₆ octahedra. A flux method is useful to control bulk properties of a material such as morphology and crystallinity.^{29–32} In the present study, we synthesized Na_{0.5}Bi_{0.5}TiO₃ of a photocatalyst VB-controlled with Bi6s orbitals by a solid state reaction and a flux method, and investigated their photocatalytic water splitting with loading suitable cocatalysts.

Na_{0.5}Bi_{0.5}TiO₃ was synthesized by a solid state reaction (SSR) and a flux method (FM) using Na₂CO₃ (Kanto Chemical; 99.8%), Bi₂O₃ (Kanto Chemical; 99.9%) and TiO₂ (Kojundo; 99.99%) as starting materials. After the starting materials were mixed in an alumina mortar in a ratio of Na₂CO₃ : Bi₂O₃ : TiO₂ = 0.25 : 0.25 : 1, the mixture was calcined at 1173–1373 K for 5 h in air for the SSR. The obtained material was washed with distilled water. For the FM, 10 molar equivalence of NaCl (Kanto Chemical; 99.5%) to the objective was used as a flux reagent. The mixture of the starting materials and the NaCl-flux was heated at 1173–1473 K for 5 h in air. The obtained material was washed with distilled water to remove the NaCl-flux. Na_{0.5}La_{0.5}TiO₃ and Na_{0.5}La_{0.25}Bi_{0.25}TiO₃ were also synthesized by FM at 1273 K for 5 h with the NaCl-flux in order to compare their band structures with Na_{0.5}Bi_{0.5}TiO₃. Details of the experiment are described in the footnotes of the Figures and Tables, and the ESI.†

X-ray diffraction (XRD) patterns revealed that Na_{0.5}Bi_{0.5}TiO₃ was successfully synthesized by SSR and FM (Fig. S2, ESI†). The FWHMs of the (012) peaks of the sample synthesized by FM at 1273–1473 K were similar to each other and smaller than those of the other samples. This result indicates that these samples synthesized by FM at 1273–1473 K possessed higher crystallinity than the other samples. The change in width of the peak split between (104) and (110) depending on the calcination temperature suggests that distortion of the perovskite framework slightly changed. The effect of synthesis method on the morphology of Na_{0.5}Bi_{0.5}TiO₃ particles was investigated by scanning electron microscopy (SEM) measurements, as shown in Fig. 1. The particle surfaces of the samples synthesized by FM were more faceted than those of the samples synthesized by SSR. Particles prepared by FM were small comparing with SSR at the same calcination temperature. The surface area (S.A.) of the samples synthesized by FM was larger than those of the samples synthesized by SSR. All absorption edges of diffuse reflectance spectra (DRS) of the Na_{0.5}Bi_{0.5}TiO₃ were located at around 400–420 nm, as shown in Fig. 2, indicating that the BG of Na_{0.5}Bi_{0.5}TiO₃ was 3.0–3.1 eV. The BG of Na_{0.5}La_{0.5}TiO₃ in which the VB is formed by O2p orbitals was estimated to be 3.4 eV from its DRS. Therefore, the BG of Na_{0.5}Bi_{0.5}TiO₃ was narrowed about 0.3 eV due to the contribution of Bi6s orbitals to its VB. The absorption edge of Na_{0.5}La_{0.25}Bi_{0.25}TiO₃ was located between those of the Na_{0.5}La_{0.5}TiO₃ and the Na_{0.5}Bi_{0.5}TiO₃ (Fig. S3, ESI†). XPS spectra at the VB regions of

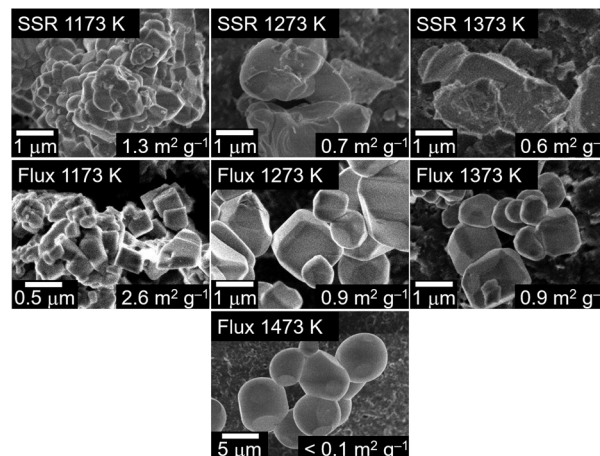


Fig. 1 SEM images and surface areas of Na_{0.5}Bi_{0.5}TiO₃ synthesized by SSR and FM at various temperatures.

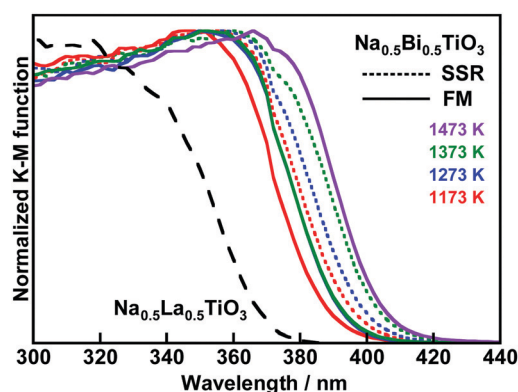


Fig. 2 Diffuse reflectance spectra of Na_{0.5}Bi_{0.5}TiO₃ synthesized by SSR and FM at various temperatures and Na_{0.5}La_{0.5}TiO₃ synthesized by FM at 1273 K.

Na_{0.5}Bi_{0.5}TiO₃ and Na_{0.5}La_{0.5}TiO₃ synthesized by FM at 1273 K were measured (Fig. S4, ESI†). The peak of the Na_{0.5}Bi_{0.5}TiO₃ was wider than that of the Na_{0.5}La_{0.5}TiO₃. The onset binding energy of the peak of the Na_{0.5}Bi_{0.5}TiO₃ shifted to a lower energy of about 0.3 eV than that of the Na_{0.5}La_{0.5}TiO₃. These results also suggest that Bi6s orbitals contributed to the valence band maximum (VBM) of the Na_{0.5}Bi_{0.5}TiO₃. DFT calculations also revealed that Bi(III) contributed to the VB of the Na_{0.5}Bi_{0.5}TiO₃.²³ The VBM formed by O2p orbitals of materials consisting of MO₆ (M = metal cation) such as Na_{0.5}La_{0.5}TiO₃ are located around +3.0 eV vs. RHE.³³ Thus, the conduction band minimum (CBM) of Na_{0.5}La_{0.5}TiO₃ was calculated to be −0.4 eV vs. RHE from its BG. CBM depends on the distortion of M–O–M bond angles.³⁴ Therefore, the CBM of Na_{0.5}Bi_{0.5}TiO₃ was also −0.4 eV vs. RHE because the Ti–O–Ti bond angle of the Na_{0.5}Bi_{0.5}TiO₃ was similar to that of the Na_{0.5}La_{0.5}TiO₃ (Table S1, ESI†). The CBM of Na_{0.5}Bi_{0.5}TiO₃ has an advantage in a driving force for reduction of water to hydrogen compared with that of SrTiO₃ (−0.2 V vs. RHE). The BG of the Na_{0.5}Bi_{0.5}TiO₃ was narrowed 0.3 eV by the contribution of Bi6s to its VBM compared with



$\text{Na}_{0.5}\text{La}_{0.5}\text{TiO}_3$, as mentioned above. The VBM of the $\text{Na}_{0.5}\text{Bi}_{0.5}\text{TiO}_3$ was calculated to be +2.7 eV from its BG and CBM. The small shift in the absorption edges seemed to be due to the difference in the distortion of the crystal structure and the particle size depending on the synthesis conditions. Additionally, the molar ratios of Bi/Ti for the samples synthesized by FM at 1173–1373 K were slightly smaller than those for the other samples (Table S2, ESI†). The smaller molar ratios of Bi/Ti for the samples synthesized by FM at 1173–1373 K also seemed to affect the difference in the absorption edges because Bi6s orbitals contributed to the VBM of $\text{Na}_{0.5}\text{Bi}_{0.5}\text{TiO}_3$.

Photocatalytic water splitting over $\text{Na}_{0.5}\text{Bi}_{0.5}\text{TiO}_3$ under UV irradiation ($\lambda > 300$ nm) was examined, as shown in Table 1. RhCr_2O_x is an excellent cocatalyst for water splitting.^{35,36} We applied the cocatalyst to the present $\text{Na}_{0.5}\text{Bi}_{0.5}\text{TiO}_3$. All samples produced H_2 and O_2 in a stoichiometric ratio. The samples synthesized by FM at 1273 and 1373 K especially showed high photocatalytic activities, because these samples possessed good crystallinity as seen in XRD (Fig. S2, ESI†). Photogenerated carriers easily migrated to the surface of such well-crystallized particles, resulting in high activities. Although the sample synthesized by FM at 1473 K possessed similar crystallinity to the samples synthesized by FM at 1273 and 1373 K, it showed a quite low activity because of its very small S.A. ($< 0.1 \text{ m}^2 \text{ g}^{-1}$). Non-loaded $\text{Na}_{0.5}\text{Bi}_{0.5}\text{TiO}_3$ synthesized by FM at 1273 K hardly showed photocatalytic activity for water splitting under UV irradiation (Table S3, ESI†). 0.1 mol% was the optimum loading amount of the RhCr_2O_x cocatalyst. Coloaded of the RhCr_2O_x cocatalyst with a CoOOH of an O_2 -evolving cocatalyst is effective for water splitting over the Al-doped SrTiO_3 photocatalyst.^{16,37} The water splitting activity of the RhCr_2O_x (0.1 mol%)-loaded $\text{Na}_{0.5}\text{Bi}_{0.5}\text{TiO}_3$ was further improved by loading of the CoOOH cocatalyst. RhCr_2O_x (0.1 mol%) and CoOOH (0.02 mol%)-coloaded $\text{Na}_{0.5}\text{Bi}_{0.5}\text{TiO}_3$ showed the highest activity for photocatalytic water splitting (Table S3 and Fig. S5, ESI†). The binding energy of the $\text{Rh}3d_{5/2}$ peak in the XPS spectrum of the RhCr_2O_x (0.1 mol%)/ $\text{Na}_{0.5}\text{Bi}_{0.5}\text{TiO}_3$ /CoOOH (0.02 mol%) (308.9 eV) was similar to not that of Rh_2O_3 (308.3 eV) but those of $\text{Rh}_{0.5}\text{Cr}_{1.5}\text{O}_3$ (0.2 mol%)/ $\text{Na}_{0.5}\text{Bi}_{0.5}\text{TiO}_3$ (308.9 eV) loaded by an impregnation method and previously reported $\text{Rh}_{2-x}\text{Cr}_x\text{O}_3$ /

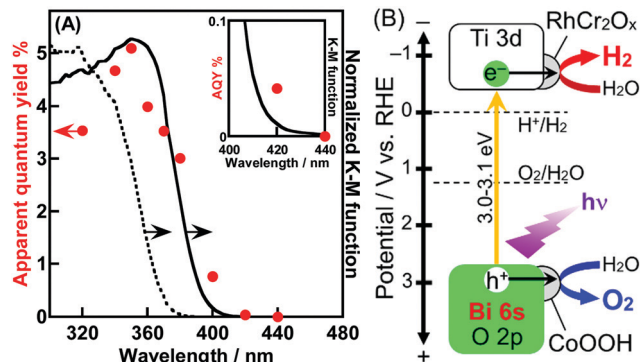


Fig. 3 (A) Action spectrum of photocatalytic water splitting over RhCr_2O_x (0.1 mol%)/ $\text{Na}_{0.5}\text{Bi}_{0.5}\text{TiO}_3$ /CoOOH (0.02 mol%), and diffuse reflectance spectra of $\text{Na}_{0.5}\text{La}_{0.5}\text{TiO}_3$ (dashed line) and $\text{Na}_{0.5}\text{Bi}_{0.5}\text{TiO}_3$ (solid line) synthesized by FM at 1273 K. Photocatalyst: 0.3 g, cocatalyst: PD, reactant solution: distilled water (120 mL), cell: top-irradiation cell with a Pyrex window, light source: 300 W Xe-arc lamp with band-pass filters. (B) Reaction scheme of photocatalytic water splitting over RhCr_2O_x (0.1 mol%)/ $\text{Na}_{0.5}\text{Bi}_{0.5}\text{TiO}_3$ /CoOOH (0.02 mol%).

$(\text{Ga}_{1-x}\text{Zn}_x)(\text{N}_{1-x}\text{O}_x)$ (309.0 eV) loaded by a simultaneous PD method (Fig. S6, ESI†).^{35,36} Therefore, the RhCr_2O_x loaded on the $\text{Na}_{0.5}\text{Bi}_{0.5}\text{TiO}_3$ was suggested to be mainly a $\text{Rh}_{2-y}\text{Cr}_y\text{O}_3$ of a mixed-oxide. The optimum $\text{Na}_{0.5}\text{Bi}_{0.5}\text{TiO}_3$ also showed much higher photocatalytic activity for water splitting than $\text{Na}_{0.5}\text{La}_{0.5}\text{TiO}_3$ and $\text{Na}_{0.5}\text{La}_{0.25}\text{Bi}_{0.25}\text{TiO}_3$ (Table S3, ESI†). This might be because photo-generated holes in the $\text{Na}_{0.5}\text{Bi}_{0.5}\text{TiO}_3$ could easily migrate to the particle surfaces because of the contribution of Bi(III) to the VB.

Fig. 3(A) shows an action spectrum of photocatalytic water splitting over the RhCr_2O_x (0.1 mol%)/ $\text{Na}_{0.5}\text{Bi}_{0.5}\text{TiO}_3$ /CoOOH (0.02 mol%). The onset wavelength of the activity agreed with that of the absorption spectrum of $\text{Na}_{0.5}\text{Bi}_{0.5}\text{TiO}_3$. This agreement indicates that water splitting proceeded with photoexcitation from the VB formed by Bi6s orbitals to the CB formed by Ti3d, as shown in Fig. 3(B). The AQY was 5.1% at 350 nm. As far as we know, among metal oxide photocatalysts with VB formed by Bi6s orbitals, the AQY is the highest for one-step photoexcitation type water splitting. Additionally, the AQY was slightly higher than that of RhCr_2O_x -loaded GaN–ZnO which shows the highest AQY among a visible-light-driven photocatalyst for water splitting.⁷ Moreover, RhCr_2O_x (0.1 mol%)/ $\text{Na}_{0.5}\text{Bi}_{0.5}\text{TiO}_3$ /CoOOH (0.02 mol%) responded to light up to 420 nm.

Water splitting proceeded over the RhCr_2O_x (0.1 mol%)/ $\text{Na}_{0.5}\text{Bi}_{0.5}\text{TiO}_3$ /CoOOH (0.02 mol%) even under simulated sunlight irradiation, as shown in Fig. 4. H_2 and O_2 steadily evolved for a long time at the rates of $203 \text{ mL h}^{-1} \text{ m}^{-2}$ and $91 \text{ mL h}^{-1} \text{ m}^{-2}$, respectively. The STH was estimated to be 0.05%. Thus, we successfully achieved one-step photoexcitation type solar water splitting using RhCr_2O_x (0.1 mol%)/ $\text{Na}_{0.5}\text{Bi}_{0.5}\text{TiO}_3$ /CoOOH (0.02 mol%) as a photocatalyst VB-controlled with Bi(III) possessing a narrower BG than SrTiO_3 .

In conclusion, $\text{Na}_{0.5}\text{Bi}_{0.5}\text{TiO}_3$, which is a photocatalyst VB-controlled with Bi(III), synthesized by a flux method at 1273 K has arisen as a new photocatalyst for solar water splitting in a suspension system when RhCr_2O_x (0.1 mol%) and CoOOH (0.02 mol%) were coloaded. $\text{Na}_{0.5}\text{Bi}_{0.5}\text{TiO}_3$ synthesized

Table 1 Photocatalytic water splitting over RhCr_2O_x (0.2 mol%)-loaded $\text{Na}_{0.5}\text{Bi}_{0.5}\text{TiO}_3$ synthesized by SSR and FM under UV irradiation

Synthesis condition		FWHM of (012) peak/ $^\circ$	S. A./ $\text{m}^2 \text{ g}^{-1}$	Activity/ $\mu\text{mol h}^{-1}$	
Method	Temp./K			H_2	O_2
SSR	1173	0.11	1.3	30	14
SSR	1273	0.10	0.7	33	16
SSR	1373	0.10	0.6	10	4.9
FM	1173	0.12	2.6	9	4
FM	1273	0.09	0.9	102	50
FM	1373	0.09	0.9	58	27
FM	1473	0.09	< 0.1	1	0.4

Photocatalyst: 0.3 g, reactant solution: distilled water (120 mL), cell: top-irradiation cell with a Pyrex window, light source: 300 W Xe-arc lamp ($\lambda > 300$ nm). A RhCr_2O_x (0.2 mol%) cocatalyst was loaded *in situ* by a photodeposition (PD) method.



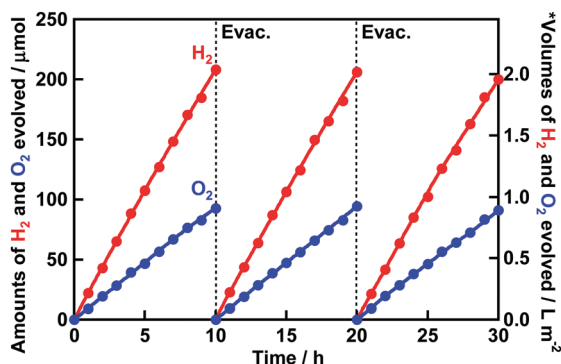


Fig. 4 Photocatalytic solar water splitting over $\text{RhCr}_2\text{O}_x(0.1 \text{ mol\%})/\text{Na}_{0.5}\text{Bi}_{0.5}\text{TiO}_3/\text{CoOOH}(0.02 \text{ mol\%})$. $\text{Na}_{0.5}\text{Bi}_{0.5}\text{TiO}_3$ was synthesized by FM at 1273 K. Photocatalyst: 0.3 g, cocatalyst: PD, reactant solution: distilled water (120 mL), cell: top-irradiation cell with a Pyrex window, light source: solar simulator (AM-1.5 G, 100 mW cm^{-2}), irradiation area: 25 cm^2 . *Volumes were calculated with the conditions of room temperature, supposing 1 atm and 1 m^2 of irradiated area.

by FM was more highly crystallized and faceted than the samples synthesized by SSR. XPS measurements revealed that the VBM of $\text{Na}_{0.5}\text{Bi}_{0.5}\text{TiO}_3$ was formed by Bi6s orbitals. The highly crystalline $\text{Na}_{0.5}\text{Bi}_{0.5}\text{TiO}_3$ with facets obtained by FM showed higher water splitting activity under UV irradiation than $\text{Na}_{0.5}\text{Bi}_{0.5}\text{TiO}_3$ obtained by SSR. This seemed to be because photogenerated carriers were able to easily migrate to the particle surfaces due to its high crystallinity. Optimized $\text{RhCr}_2\text{O}_x(0.1 \text{ mol\%})/\text{Na}_{0.5}\text{Bi}_{0.5}\text{TiO}_3/\text{CoOOH}(0.02 \text{ mol\%})$ responded to light up to 420 nm. This photocatalyst gave 5.1% AQY at 350 nm and 0.05% STH. The AQY and STH were the highest among photocatalysts VB-controlled with Bi(III). Thus, we have demonstrated solar water splitting *via* one-step type photoexcitation using a VB-controlled photocatalyst consisting of Bi(III) with a narrower BG than SrTiO_3 .

This work was supported by JSPS KAKENHI Grant Numbers 17H06433 and 17H06440 in Scientific Research on Innovative Areas “Innovations for Light-Energy Conversion (I⁴LEC)”, and 17H01217.

Conflicts of interest

There are no conflicts to declare.

References

- 1 F. E. Osterloh, *Chem. Mater.*, 2008, **20**, 35–54.
- 2 Y. Inoue, *Energy Environ. Sci.*, 2009, **2**, 364–386.
- 3 A. Kudo and Y. Miseki, *Chem. Soc. Rev.*, 2009, **38**, 253–278.
- 4 R. Abe, *J. Photochem. Photobiol. C*, 2010, **11**, 179–209.

- 5 T. Hisatomi, J. Kubota and K. Domen, *Chem. Soc. Rev.*, 2014, **43**, 7520–7535.
- 6 K. Maeda and K. Domen, *Bull. Chem. Soc. Jpn.*, 2016, **89**, 627–648.
- 7 K. Maeda, K. Teramura, D. Lu, T. Takata, N. Saito, Y. Inoue and K. Domen, *Nature*, 2006, **440**, 295.
- 8 Y. Lee, H. Terashima, Y. Shimodaira, K. Teramura, M. Hara, H. Kobayashi, K. Domen and M. Yashima, *J. Phys. Chem. C*, 2007, **111**, 1042–1048.
- 9 C. Pan, T. Takata, M. Nakabayashi, T. Matsumoto, N. Shibata, Y. Ikumura and K. Domen, *Angew. Chem., Int. Ed.*, 2015, **54**, 2955–2959.
- 10 K. Maeda, D. Lu and K. Domen, *Chem. – Eur. J.*, 2013, **19**, 4986–4991.
- 11 J. Xu, C. Pan, T. Takata and K. Domen, *Chem. Commun.*, 2015, **51**, 7191–7194.
- 12 Z. Wang, Y. Inoue, T. Hisatomi, R. Ishikawa, Q. Wang, T. Takata, S. Chen, N. Shibata, Y. Ikumura and K. Domen, *Nat. Catal.*, 2018, **1**, 756–763.
- 13 Q. Wang, M. Nakabayashi, T. Hisatomi, S. Sun, S. Akiyama, Z. Wang, Z. Pan, X. Xiao, T. Watanabe, T. Yamada, N. Shibata, T. Takata and K. Domen, *Nat. Mater.*, 2019, **18**, 827–832.
- 14 G. Zhang, Z.-A. Lan, L. Lin, S. Lin and X. Wang, *Chem. Sci.*, 2016, **7**, 3062–3066.
- 15 R. Asai, H. Nemoto, Q. Jia, K. Saito, A. Iwase and A. Kudo, *Chem. Commun.*, 2014, **50**, 2543–2546.
- 16 T. Takata, J. Jiang, Y. Sakata, M. Nakabayashi, N. Shibata, V. Nandal, K. Seki, T. Hisatomi and K. Domen, *Nature*, 2020, **581**, 411–414.
- 17 K. Watanabe, A. Iwase and A. Kudo, *Chem. Sci.*, 2020, **11**, 2330–2334.
- 18 H. Kato, H. Kobayashi and A. Kudo, *J. Phys. Chem. B*, 2002, **106**, 12441–12447.
- 19 A. Kudo, H. Kato and I. Tsuji, *Chem. Lett.*, 2004, **33**, 1534–1539.
- 20 A. Kudo, K. Omori and H. Kato, *J. Am. Chem. Soc.*, 1999, **121**, 11459–11467.
- 21 H. Kato, N. Matsudo and A. Kudo, *Chem. Lett.*, 2004, **33**, 1216–1217.
- 22 A. Kudo and S. Hiji, *Chem. Lett.*, 1999, 1103–1104.
- 23 M. Zeng, S. W. Or and H. L. W. Chan, *J. Appl. Phys.*, 2010, **107**, 043513.
- 24 Y. Iikubo, H. Kato and A. Kudo, *Abstract of 94th CATSJ Meeting, 2004, P038*; Y. Iikubo, MPhil thesis, Tokyo University of Science, 2005.
- 25 L. Wang and W. Wang, *Int. J. Hydrogen Energy*, 2012, **37**, 3041–3047.
- 26 Z. Ai, G. Lu and S. Lee, *J. Alloys Compd.*, 2014, **613**, 260–266.
- 27 R. Zhang, X. Wu, Y. Li, W. Shao, Y. Zhang, Z. Liu, J. Nie, J. Tan and W. Ye, *RSC Adv.*, 2020, **10**, 7443–7451.
- 28 Y. Ham, T. Hisatomi, Y. Goto, Y. Moriya, Y. Sakata, A. Yamakata, J. Kubota and K. Domen, *J. Mater. Chem. A*, 2016, **4**, 3027–3033.
- 29 X. Liu, N. Fechner and M. Antonietti, *Chem. Soc. Rev.*, 2013, **42**, 8237–8265.
- 30 Q. Wang, Q. Guo, L. Wang and B. Li, *Dalton Trans.*, 2016, **45**, 17748–17758.
- 31 Q. Wang, B. Zhang, X. Lu, X. Zhang, H. Zhu and B. Li, *Catal. Sci. Technol.*, 2018, **8**, 6180–6195.
- 32 J. Boltersdorf, N. King and P. A. Maggard, *CrystEngComm*, 2015, **17**, 2225–2241.
- 33 D. E. Scaife, *Sol. Energy*, 1980, **25**, 41–54.
- 34 H. Kato and A. Kudo, *J. Phys. Chem. B*, 2001, **105**, 4285–4292.
- 35 K. Maeda, D. Lu, K. Teramura and K. Domen, *J. Mater. Chem.*, 2008, **18**, 3539–3542.
- 36 K. Maeda, D. Lu, K. Teramura and K. Domen, *Energy Environ. Sci.*, 2010, **3**, 470–477.
- 37 H. Lyu, T. Hisatomi, Y. Goto, M. Yoshida, T. Higashi, M. Katayama, T. Takata, T. Minegishi, H. Nishiyama, T. Yamada, Y. Sakata, K. Asakura and K. Domen, *Chem. Sci.*, 2019, **10**, 3196–3201.

